Interacting RNA polymerase motors on DNA track:
effects of traffic congestion and intrinsic noise on RNA synthesis

Tripti Tripathi[1] and Debashish Chowdhury[2]

[1]*Physics Department, Indian Institute of Technology, Kanpur 208016, India*
[2]*Physics Department, Indian Institute of Technology, Kanpur 208016, India, and*
Max-Planck Institute for Physics of Complex Systems, 01187 Dresden, Germany[*]
(Dated: August 17, 2007)

RNA polymerase (RNAP) is an enzyme that synthesizes a messenger RNA (mRNA) strand which is complementary to a single-stranded DNA template. From the perspective of physicists, an RNAP is a molecular motor that utilizes chemical energy input to move along the track formed by a DNA. In many circumstances, which are described in this paper, a large number of RNAPs move simultaneously along the same track; we refer to such collective movements of the RNAPs as RNAP traffic. Here we develop a theoretical model for RNAP traffic by incorporating the steric interactions between RNAPs as well as the mechano-chemical cycle of individual RNAPs during the elongation of the mRNA. By a combination of analytical and numerical techniques, we calculate the rates of mRNA synthesis and the average density profile of the RNAPs on the DNA track. We also introduce, and compute, two new measures of fluctuations in the synthesis of RNA. Analyzing these fluctuations, we show how the level of *intrinsic noise* in mRNA synthesis depends on the concentrations of the RNAPs as well as on those of some of the reactants and the products of the enzymatic reactions catalyzed by RNAP. We suggest appropriate experimental systems and techniques for testing our theoretical predictions.

PACS numbers: 87.16.Ac 89.20.-a

I. INTRODUCTION

Molecular motors [1, 2, 3] are either proteins or macromolecular complexes that utilize some form of input energy (often chemical energy) to perform mechanical work. In many circumstances, molecular motors move collectively on a single track in a manner that has strong resemblance with vehicular traffic [4, 5]. In recent years some minimal models of molecular motor traffic have been developed to study their generic features [6, 7, 8, 9]. More detailed models for specific motor traffic systems have also been proposed by capturing the stochastic mechano-chemistry of individual motors as well as their steric interactions within the same model to investigate the interplay of individual and collective dynamics of the motors [10, 11, 12]. In this paper we develop such a model for a specific class of motors for which no attempt has been made in the past to capture their steric interactions during traffic-like collective movements on a single track.

According to the central dogma of molecular biology, the genetic message stored in the DNA is first *transcribed* into messenger RNA (mRNA) from which it is then *translated* into proteins. Polymerization of a mRNA from the corresponding single-stranded DNA (ssDNA) template is carried out by a motor called RNA polymerase (RNAP) [13, 14, 15]. A ribosome is a motor that synthesizes a protein from the corresponding mRNA template. The steric interactions were taken into account in most of the theoretical models of translation developed since the late sixties [10, 16, 17, 18, 19, 20, 21, 22, 23, 24]. Surprisingly, in spite of the close similarities between the template-dictated and motor-driven polymerization of macromolecules in transcription and translation, no attempt has been made in the past to incorporate interactions of RNAPs in the theoretical description of transcription. Instead, to our knowledge, all the models of transcription reported so far [25, 26, 27, 28, 29, 30, 31, 32, 33, 34, 35] capture only the stochatic mechano-chemistry of the individual RNAP motors. Cooperation and collisions between RNAP motors is known to have non-trivial effects on the rate of transcription [36, 37, 38, 39]. Moreover, the possibility of the formation of queues in RNAP traffic has also been explored [40]. In fact, if the gene is relatively short, a sufficiently long queue of RNAPs on the ssDNA template can reduce the accessibility of the promoter sequence thereby lowering the rate of further initiation of transcription.

The main aim of this paper is to develop a model of RNAP traffic that incorporates steric interactions between RNAP motors which move along the same DNA track. In this model, we incorporate the most essential features of the multi-step mechano-chemical pathway of the individual RNAP motors by a scheme which was used earlier in Wang et al.'s [26] model for single RNAP. The steric interaction between the RNAPs is assumed to be hard-core repulsion. The effects of these interactions of RNAPs is captured in our model of mRNA synthesis in the same manner in which the steric interactions of ribosomes was captured in a recent model [10] of protein synthesis.

In the spirit of traffic science [41], we define the *flux* to be the average number of motors crossing a site per unit

time. Thus, flux is expressed in the units "number per second". We define the number density to be the average number of RNAPs attached to unit length of the ssDNA template. Using the terminology of traffic science, we refer to the relation between the flux and the number density of the RNAPs as the *fundamental diagram*. We calculate the flux and investigate its dependence on the number density of RNAP on the ssDNA template as well as on some other experimentally accessible parameters of the model. Since average speed of a RNAP is also a measure of the average rate of mRNA elongation and the flux gives the total rate of mRNA synthesis from a ssDNA template, our calculations predict the effects of RNAP traffic congestion on the rate of synthesis of mRNA.

The steps of the mechano-chemical cycle of a RNAP are intrinsically stochastic and give rise to fluctuations in the rates of synthesis of mRNA. We introduce quantitative measures of these fluctuations by drawing analogy with some further concepts from traffic science [41]. We define the *run time T* of a RNAP to be the actual time it takes to travel from the start site to the stop site on the DNA template (i.e., the time taken to synthesize an mRNA transcript). Similarly, we define the *time-headway τ* to be the time interval between the departures of two successive RNAPs from the stop site on the DNA template (i.e., the time interval between the completion of the synthesis of successive mRNA transcripts). Using the stochastic model which we develope here for RNAP traffic, we also compute the distributions $\tilde{P}_T$ and $\mathcal{P}_\tau$ of run-times and time-headways respectively.

In recent years, stochasticity in gene expression has been probed by novel experimental techniques and the results have inspired several theoretical models at different levels of complexity [42]. The cell-to-cell variations in the levels of expression of the same gene can arise from inherently *intrinsic* fluctuations in transcription and translation or from *extrinsic* causes [43]. Since proteins are the final products of gene expression, normally, fluctuations in the concentration of proteins are taken as a measure of the noise in gene expression. However, the most direct way to measure transcriptional noise would be to monitor the fluctuations in the synthesis of mRNA transcripts [44, 45, 46, 47]. Therefore, instead of modeling cell-to-cell variations in the transcription of a specific gene, in this paper we study the *RNAP-to-RNAP fluctuations* in the synthesis of mRNA from a *single DNA template*. The width of the distributions $\tilde{P}_T$ and $\mathcal{P}_\tau$ provide measures

of the contributions to *transcriptional noise* from the intrinsic fluctuations in the steps of the mechano-chemical cycle of RNAPs on the same DNA template.

The paper is organized as follows. In section II we summarize the essential mechano-chemical processes involved in transcription. In the same section we also present a brief review of some of the relevant earlier models. Our stochastic model is developed in section III. Our theoretical predictions on flux and average density profiles, which follow from this model under periodic and open boundary conditions, are discussed in the sections IV and V, respectively. Our results on fluctuations and transcriptional noise are presented in section VI. The experimental implications of our theoretical predictions are discussed in section VII. Finally, in section VIII we summarize our main theoretical predictions.

II. BRIEF REVIEW OF PHENOMENOLOGY AND EARLIER MODELS

A. Essential chemo-mechanical processes

Transcription, i.e., the process of synthesis of mRNA from the corresponding ssDNA template, can be broadly divided into three stages, namely, *initiation*, *elongation* and *termination*. In the initiation stage, an RNAP recognizes the so-called "promoter sequence" on the DNA and locally unzips the two DNA strands creating a "bubble" whereby a ssDNA template is exposed to it. However, in this paper we are interested mainly in the elongation of the mRNA transcript.

During elongation [48], each successful addition of a nucleotide to the elongating mRNA leads to a forward stepping of the RNAP. The RNAP, together with the DNA bubble and the growing RNA transcript, forms a "transcription elongation complex" (TEC). Each mechano-chemical cycle of the RNAP during the elongation stage [13, 49, 50] consists of several steps; the major steps being (i) NTP binding to the active site of the RNAP when the active site is located at the growing tip of the mRNA transcript, (ii) NTP hydrolysis, (iii) release of PP_i, one of the products of hydrolysis, and (iv) accompanying forward stepping of the RNAP [13]. This simplified scenario, which is adequete for our purpose here, is shown symbolically in equation (1):

$$TEC_n + NTP \rightleftharpoons TEC_n \bullet NTP \rightleftharpoons TEC_{n+1} \bullet PP_i \rightleftharpoons TEC_{n+1} \tag{1}$$

The elongation process ends when the TEC encounters the corresponding "termination sequence" and the

nascent mRNA is released by the RNAP.

B. Brief review of the earlier models

A stochastic chemical kinetic model was developed by Jülicher and Bruinsma [25] to describe not only the polymerization of mRNA by a RNAP, but also to account for the effects of elastic strain in the motor. Almost simultaneously, Wang et al.[26] developed a model that incorporated the multi-step chemical kinetics of the transcription elongation process. Extending Von Hippel's [51, 52, 53] pioneering works on sequence-dependent thermodynamic analysis of transcription, Wang and collaborators [13, 30] have developed a sequence-dependent kinetic model in terms of a transcription-energy landscape. This model has been extended further by Tadigotla et al. [33] by incorporating the kinetic barriers erected by the folding of the mRNA transcript. Very recently, Bai et al.[31] have demonstrated the predictive power of their theoretical model carrying out experiment and data analysis in two stages: in the first they estimated the model parameters from experimental exploration of the response to *chemical* perturbations, and, then, in the second stage using these parameters they predicted the responses to *mechanical* perturbations. But, as stated in the introduction, none of these models incorporate steric interactions between the RNAPs.

To our knowledge, the first model of molecular motor traffic was developed almost forty years ago by MacDonald, Gibbs and collaborators [16, 17] in the context of ribosome traffic. The details of molecular composition and achitecture as well as the mechano-chemical cycles of the ribosomes were not taken into account in these pioneering works. Instead, each ribosome was modelled as a hard rod; in the special limit where the size of the rod coincides with the lattice constant, this model reduces to the totally asymmetric simple exclusion process (TASEP) which is the simplest model of interacting self-propelled particles. Very recently, a more realistic model [10] of ribosome traffic has been developed by incorporating the essenial steps in the mechano-chemical cycle of a ribosome during the elongation of the protein. Traffic of some other families of motors have also been modelled recently in the same spirit, i.e., by incorporating both the intra-motor mechano-chemistry and inter-motor steric interactions [11].

III. MODEL

We represent the ssDNA template by a one-dimensional lattice (see fig.1). We label the sites of the lattice by the integer index i (by convention, from left to right). The sites $i = 1$ and $i = L$ represent the start and stop sites, respectively. Each of the remaining sites in between the start and stop sites (i.e., $2 \leq i \leq L - 1$) represents a single nucleotide on the ssDNA template. The size of a single RNAP is such that each motor can simultaneously cover r successive nucleotides on the ssDNA template (usually, r is typically 30 base pairs, but
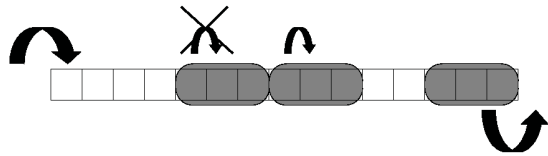

FIG. 1: A schematic representation of the model. The ssDNA template is assumed to be an, effectively, one-dimensional track for the RNAP motors. This track is discretized schematically by the array of the (imaginary) boxes. The positions of the sites on the lattice formed by the midpoints of these boxes represents the positions of the nucleotides on the ssDNA template. Each dark rectangle represents a RNAP that can cover r sites simultaneously ($r = 3$ in this figure).

in fig1 $r = 3$). According to our convention, the position of each RNAP is denoted by the integer index of the lattice site covered by the leftmost site of the RNAP. Thus, the allowed range of the positions j of each RNAP is $1 \leq j \leq L$. The hard-core steric interactions among the RNAPs is captured by imposing the condition that no lattice site is allowed to be covered simultaneously by more than one RNAP. Irrespective of the actual numerical value of r, each RNAP can move forward or backward by only one site in each time step, if demanded by its own mechano-chemistry, provided the target site is not already covered by any other RNAP. This is motivated by the fact that a RNAP must transcribe the successive nucleotides one by one.

The total number of RNAPs on the ssDNA template is denoted by the symbol N. Under periodic boundary conditions (PBC), N is independent of time whereas N is a fluctuating time-dependent quantity if open boundary conditions (OBC) are imposed on the system. Therefore, $\rho = N/L$ is the *number density* of the RNAPs. The *coverage density* is defined by $\rho_{cov} = Nr/L$ which is the total fraction of the nucleotides covered by all the RNAPs together. Under OBC, the number density as well as the coverage density are, in general, fluctuating quantities, but the average of these densities attain time-independent values in the stationary state.

Our model is aimed at the elongation stage and is not intended to describe the initiation and termination processes in detail. Therefore, we represent initiation and termination by the two parameters α and β, respectively. Whenever the site $i = 1$ on the ssDNA template is vacant, this site is allowed to be occupied by a new RNAP
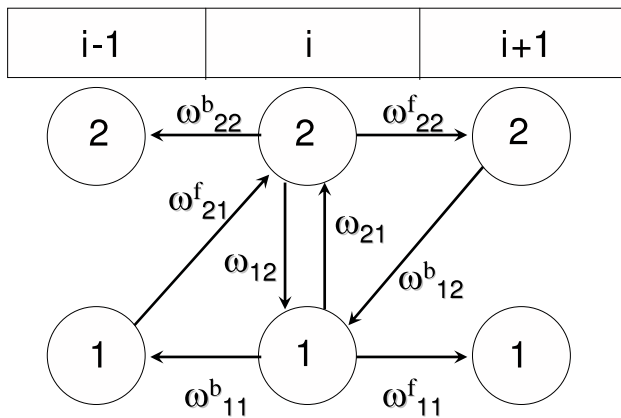
FIG. 2: A schematic representation of the mechano-chemical cycle of each RNAP in our model in the elongation stage. No PP_i is bound to the RNAP in the state 1 whereas the PP_i-bound state of the RNAP is labelled by the index 2.

with the probability α in the time interval Δt (in all our numerical calculations we take $\Delta t = 0.001s$). Similarly, a RNAP bound to the site $i = L$ is allowed to detach from the template with the probability β in the time interval Δt. For convenience, we also define the probabilities ω_α and ω_β for attachment and detachment, respectively. Note that ω_α is related to α by the relation $\alpha = 1 - exp(-\omega_\alpha \Delta t)$; ω_β is related to β by a similar relation.

Following Wang et al.[26], we have a simplified description of the chemical (or, conformational) states of each individual RNAP. Since release of PP_i is the rate limiting step in the process of elongation of the mRNA transcript, we consider only two, effectively distinct, chemical states of the RNAP in each mechano-chemical cycle during the elongation stage. In the state labelled by the integer index 1 no PP_i is bound to the RNAP whereas the PP_i-bound state of the RNAP is labelled by the index 2. The simplified scheme, that captures the essential mechano-chemical processes during the mRNA transcript elongation, is shown in fig.2 . In this figure, ω_{21}^f, ω_{11}^f and ω_{22}^f are the rates of polymerization of RNA in three diferrent situations, namely, by the hydrolysis of nucleotides (i) on the RNAP, (ii) in solution (while no PP_i is bound to the RNAP and (iii) in solution, while PP_i is bound to the RNAP. The corresponding rates of reverse transitions, which result in depolymerization of the RNA, are denoted by the symbols ω_{12}^b, ω_{11}^b and ω_{22}^b, respectively. Finally, ω_{21} and ω_{12} are the rates of association and dissociation, respectively, of PP_i.

The single-RNAP mechano-chemistry in our model does not capture the well known phenomena of RNAP "backtracking" and "hypertracking" which are observed in *in-vitro* single-RNAP experiments [54, 55]. But, it has been experimentally demonstrated [36, 37] that backtracking of a RNAP gets strongly suppressed if there is another RNAP close behind it. Therefore, except at ex-

tremely low densities of RNAPs, backtrackings and hypertrackings are not expected to make significant contribution in the context of RNAP traffic.

Let $P_\mu(i, t)$ denote the probability that there is a RNAP at the spatial position i and in the chemical state μ at time t; $\mu = 1$ refers to the state in which the RNAP is not bound to any PP_i whereas $\mu = 2$ corresponds to the state with bound PP_i. Note that $P(i) = \sum_{\mu=1}^{2} P_\mu(i)$ is the probability of finding a RNAP at the site i, irrespective of its chemical state. Similarly, $P_\mu = \sum_i P_\mu(i)$ is the probability of finding a RNAP in the chemical state μ irrespective of its spatial position. We describe the stochastic dynamics of the system in terms of master equations for $P_\mu(i, t)$. Most of our analytical results have been derived using the mean-field approximation.

In order to test the range of validity of our approximate analytical calculations, we have also carried out extensive computer simulations of our model. In these simulations, we have used random sequential updating which appropriately corresponds to the Master equations used in our analytical formalisms. In each run of the simulations, the system was allowed to reach steady state in the first one million time steps and the data for the steady-state were collected over the next eight million time steps. The entire process was repated with large number of different initial conditions and, finally, average steady-state flux was computed. We have observed that the qualitative features of our results do not depend significantly on the actual numerical value of r as long as is sufficiently larger than unity. Therefore, unless stated otherwise, all the numerical results plotted in this paper have been obtained taking $r = 10$. In our test simulation runs, we did not find any significant variations in the data for $L \geq 1000$. Therefore, almost all the simulation data reported here were generated in our production runs by keeping L fixed at $L = 1000$.

IV. RNAP TRAFFIC UNDER PERIODIC BOUNDARY CONDITIONS

We always denote the spatial position of a RNAP on the DNA track by the integer index of the site covered by the left edge of the RNAP (i.e., the leftmost of the r successive sites representing the RNAP). Thus, in our terminology, a site is *occupied* by a RNAP if it coincides with the leftmost of the r sites representing that RNAP while the next $r-1$ sites on its right are said to be *covered* by the same RNAP.

Let $P(\underline{i}|j)$ be the conditional probability that, given a RNAP at site i, there is another RNAP at site j. Obviously, $Q(\underline{i}|j)$ is the conditional probability that, given a RNAP at site i, site j is empty. Note that, if site i is given to be occupied by one RNAP, the site $i - 1$ can be covered by another RNAP if, and only if, the site $i - r$ is also occupied.

A. Mean-field theory under periodic boundary conditions

In the mean-field approximation, the master equations for $P_\mu(i, t)$ are given by

$$
\begin{aligned}
\frac{dP_1(i,t)}{dt} &= \omega_{11}^b \, P_1(i+1,t) \, Q(i+1-r|\underline{i+1}) + \omega_{11}^f \, P_1(i-1,t) \, Q(\underline{i-1}|i-1+r) + \omega_{12}^b \, P_2(i+1,t) \, Q(i+1-r|\underline{i+1}) \\
&+ \omega_{12} \, P_2(i,t) - \omega_{21} \, P_1(i,t) - \omega_{11}^f \, P_1(i,t) \, Q(\underline{i}|i+r) - \omega_{21}^f \, P_1(i,t) \, Q(\underline{i}|i+r) - \omega_{11}^b \, P_1(i,t) \, Q(i-r|\underline{i}) \quad (2)
\end{aligned}
$$

$$
\begin{aligned}
\frac{dP_2(i,t)}{dt} &= \omega_{22}^b \, P_2(i+1,t) \, Q(i+1-r|\underline{i+1}) + \omega_{22}^f \, P_2(i-1,t) \, Q(\underline{i-1}|i-1+r) + \omega_{21}^f \, P_1(i-1,t) \, Q(\underline{i-1}|i-1+r) \\
&+ \omega_{21} P_1(i,t) - \omega_{12} \, P_2(i,t) - \omega_{22}^f \, P_2(i,t) \, Q(\underline{i}|i+r) - \omega_{12}^b \, P_2(i,t) \, Q(i-r|\underline{i}) - \omega_{22}^b \, P_2(i,t) \, Q(i-r|\underline{i}) \quad (3)
\end{aligned}
$$

Note that the two equations (2) and (3) are not independent of each other because of the condition

$$
P(i) = P_1(i) + P_2(i) = \frac{N}{L} = \rho \qquad (4)
$$

For our numerical calculations, we choose the same set of rate constants which Wang et al.[26] extracted from empirical data; these are as follows:

$$
\begin{aligned}
\omega_{21}^f &= \omega_{21}^{f0} \cdot [NTP], \text{ with } \omega_{21}^{f0} = 10^6 \ M^{-1} \cdot s^{-1} \\
\omega_{11}^f &= \omega_{11}^{f0} \cdot [NMP], \text{ with } \omega_{11}^{f0} = 46.6 \ M^{-1} \cdot s^{-1} \\
\omega_{22}^f &= \omega_{22}^{f0} \cdot [NMP], \text{ with } \omega_{22}^{f0} = 0.31 \ M^{-1} \cdot s^{-1} \\
\omega_{21} &= \omega_{21}^0 \cdot [PP_i], \text{ with } \omega_{21}^0 = 10^6 \ M^{-1} \cdot s^{-1} \\
\omega_{12} &= 31.4 \ s^{-1} \\
\omega_{12}^b &= 0.21 \ s^{-1} \\
\omega_{11}^b &= 9.4 \ s^{-1} \\
\omega_{22}^b &= 0.063 \ s^{-1}
\end{aligned}
$$
$$(5)$$

Compared to Basu and Chowdhury's model [10] of ribosome-driven protein synthesis, our model of RNAP-driven mRNA synthesis involves fewer chemical states and, hence, fewer master equations. In fact, the number of chemical states in this model is equal to those in an earlier model of traffic of single-headed kinesin motors [11, 12] where the two chemical states, however, have totally different physical interpretations. But, the number of terms involved in each of the master equations 2 and 3 are much larger than those in ref.[10] and in ref.[11, 12].

B. Steady state properties under periodic boundary conditions

In the steady state all $P_\mu(i, t)$ become indepent of time. Moreover, because of the PBC, these probabilities are also independent of the site index i in the steady state of the system. Therefore, from Bayes's theorem,

$$
\begin{aligned}
P(\underline{i}|i+r) &= \frac{P(i|\underline{i+r})P(i+r)}{P(i)} \\
&= P(i|\underline{i+r}) \qquad (6)
\end{aligned}
$$

and, hence,

$$
Q(\underline{i}|i+r) = Q(i|\underline{i+r}). \qquad (7)
$$

We calculate $Q(\underline{i}|i+r)$ along the same line as sketched in ref.[10]. Given that the site i is occupied, the conditional probability that the site $i+r$ is also occupied is given by

$$
P(\underline{i}|i+r) = \frac{N-1}{L+N-Nr-1}. \qquad (8)
$$

Thus, in the limit $L \to \infty$ and $N \to \infty$, while keeping $\rho = N/L$ fixed, we get

$$
Q(\underline{i}|i+r) = Q(i|\underline{i+r}) = \frac{1-\rho r}{1+\rho-\rho r} \qquad (9)
$$

Note that Q vanishes at $\rho = 1/r$, because the entire stretch of the ssDNA template between the points of initiation and termination of transcription is fully covered by the RNAPs at $\rho r = \rho_{cov} = 1$.

Solving Eqs.(2), together with (4) in the steady state under PBC, we get

$$
P_1 = \left(\frac{\omega_{12} + \omega_{12}^b Q}{\Omega_\updownarrow + \Omega_\leftrightarrow Q}\right) \rho
$$

$$
P_2 = \left(\frac{\omega_{21} + \omega_{21}^f Q}{\Omega_\updownarrow + \Omega_\leftrightarrow Q}\right) \rho \qquad (10)
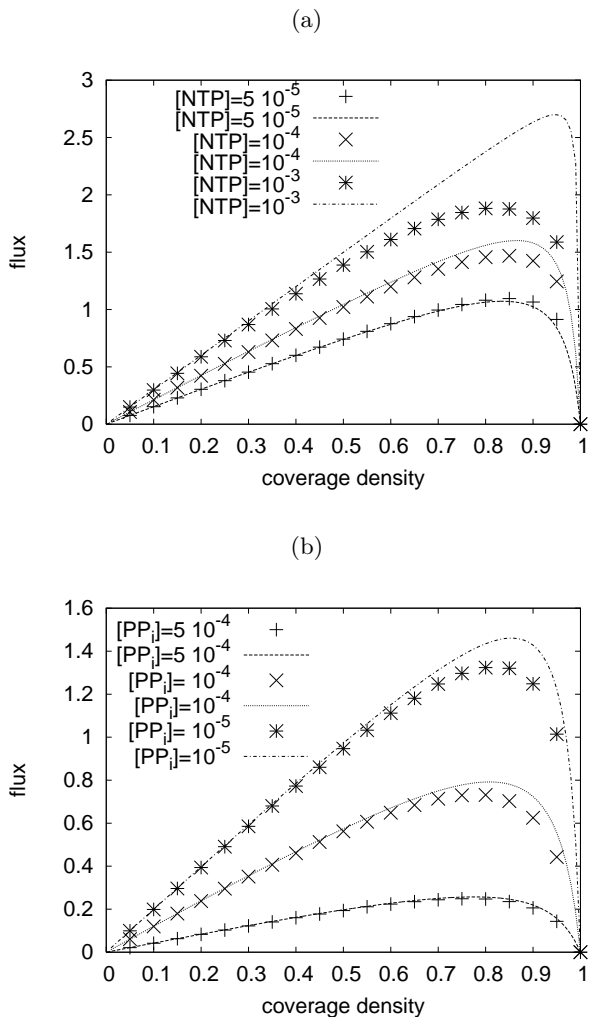$$

(a)

(b)

FIG. 3: The steady-state flux of the RNAPs, under periodic boundary conditions, plotted as a function of the coverage density ρ_{cov} for (a) three different values of [NTP] at $[PP_i] = 1\,\mu M$, and (b) three different values of $[PP_i]$ at [NTP] = 1 mM. The lines correspond to our mean-field theoretic predictions whereas the discrete data points have been obtained from computer simulations.

where

$$\Omega_{\updownarrow} = \omega_{12} + \omega_{21}$$
$$\Omega_{\leftrightarrow} = \omega_{21}^f + \omega_{12}^b \tag{11}$$

and Q is given by the equation (9).

In the steady state under PBC, the flux of the RNAPs is given by

$$J = (\omega_{11}^f + \omega_{21}^f)\, P_1\, Q(\underline{i}|i+r) + \omega_{22}^f\, P_2\, Q(\underline{i}|i+r)$$
$$- \omega_{11}^b\, P_1\, Q(i-r|\underline{i}) - (\omega_{22}^b + \omega_{12}^b)\, P_2\, Q(i-r|\underline{i}) \tag{12}$$

Hence,

$$J = \Omega_1\, P_1\, Q + \Omega_2\, P_2\, Q \tag{13}$$
$$= (\Omega_1\, P_1 + \Omega_2\, P_2)\left(\frac{1-\rho_{cov}}{1+\rho-\rho_{cov}}\right) \tag{14}$$
$$\tag{15}$$

where

$$\Omega_1 = \omega_{11}^f + \omega_{21}^f - \omega_{11}^b$$
$$\Omega_2 = \omega_{22}^f - \omega_{12}^b - \omega_{22}^b, \tag{16}$$

are two *effective forward hopping rates* from the states 1 and 2, respectively, while Q is given by the equation (9). Since $P_1 = 0 = P_2$ at $\rho = 0$ the corresponding flux J vanishes. J also vanishes at $\rho_{cov} = 1$ as Q vanishes at $\rho r = 1$.

Our mean-field estimate (15) of flux J is plotted against the coverage density ρ_{cov} in fig.3 for (a) three different values of $[NTP]$ at $[PP_i] = 1\mu M$, and (b) three different values of $[PP_i]$ at $[NTP] = 1mM$. The qualitative features of these fundamental diagrams are similar to those observed earlier [10] in the context of ribosomal traffic during protein synthesis from a mRNA template. The most notable feature of these diagrams is their *asymmetric shape*. This shape of the fundamental diagram is in sharp contrast to the symmetry of the fundamental diagram of TASEP about $\rho = 1/2$. The physical reason for the asymmetric shape of the fundamental diagram in fig.3 is the same as in ribosomal traffic [10].

The rate constant ω_{21}^f is higher at higher concentrations of NTP and gives rise to higher flux, i.e., higher rate of transcriptional output (see fig.3). Conversely, higher concentration of PP_i opposes the release of PP_i thereby slowing down the overall rate of transcription. Moreover, at higher concentrations of NTP each RNAP attempts forward stepping more frequently; while making these attempts, it feels stronger hindrance at higher densities of RNAPs. Therefore, the deviation of the mean-field estimates of flux from the corresponding simulation data is larger at higher NTP concentration and at higher coverage density of the RNAPs. Similarly, forward stepping of a RNAP is less suppressed when the PP_i concentration in the solution is lower; therefore, stronger devitation of the mean-field estimates of flux from the corresponding simulation data is observed at lower PP_i conentration and higher RNAP densities.

V. RESULTS UNDER OPEN BOUNDARY CONDITIONS

Open boundary conditions are more realistic than PBC for describing RNAP traffic during transcription. A fresh RNAP can attach with the site $i = 1$ only in the state 1 (i.e., no PPi is bound to it). In this section we make a further assumption for simplifying the equations. We

replace the conditional probability $Q(\underline{i}|j)$, by the probability $Q(j)$ that site j is empty, irrespective of the state of occupation of any other site. Note that the probability of finding a "hole" at j (i.e., the probability that the site j is not "covered" by any RNAP) is given by $1 - \sum_{s=0}^{r-1} P(j-s)$.

A. Mean-field theory under open boundary conditions

Under mean-field approximation, the master equations for the probabilities are now given by

$$
\begin{aligned}
\frac{dP_1(1,t)}{dt} =\ & \omega_\alpha \left(1 - \sum_{s=1}^{r} P(s)\right) + \omega_{11}^b \, P_1(2,t) + \omega_{12}^b \, P_2(2,t) + \omega_{12} \, P_2(1,t) \\
& - \omega_{21} \, P_1(1,t) - (\omega_{11}^f + \omega_{21}^f) \, P_1(1,t) \left(\frac{1 - \sum_{s=1}^{r} P(1+s)}{1 - \sum_{s=1}^{r} P(1+s) + P(1+r)} \right)
\end{aligned}
\tag{17}
$$

$$
\begin{aligned}
\frac{dP_1(i,t)}{dt} =\ & \left[\omega_{11}^b \, P_1(i+1,t) + \omega_{12}^b \, P_2(i+1,t) \right] \left(\frac{1 - \sum_{s=1}^{r} P(i+1-s)}{1 - \sum_{s=1}^{r} P(i+1-s) + P(i+1-r)} \right) \\
& + \omega_{11}^f \, P_1(i-1,t) \left(\frac{1 - \sum_{s=1}^{r} P(i-1+s)}{1 - \sum_{s=1}^{r} P(i-1+s) + P(i-1+r)} \right) + \omega_{12} \, P_2(i,t) \\
& - \omega_{21} \, P_1(i,t) - (\omega_{11}^f + \omega_{21}^f) \, P_1(i,t) \left(\frac{1 - \sum_{s=1}^{r} P(i+s)}{1 - \sum_{s=1}^{r} P(i+s) + P(i+r)} \right) \\
& - \omega_{11}^b \, P_1(i,t) \left(\frac{1 - \sum_{s=1}^{r} P(i-s)}{1 - \sum_{s=1}^{r} P(i-s) + P(i-r)} \right) \qquad (i \neq L, i \neq 1)
\end{aligned}
\tag{18}
$$

$$
\begin{aligned}
\frac{dP_1(L,t)}{dt} =\ & \omega_{11}^f \, P_1(L-1,t) \left(\frac{1 - \sum_{s=1}^{r} P(L-1+s)}{1 - \sum_{s=1}^{r} P(L-1+s) + P(L-1+r)} \right) + \omega_{12} \, P_2(L,t) \\
& - \omega_{21} \, P_1(L,t) - \omega_{11}^b \, P_1(L,t) \left(\frac{1 - \sum_{s=1}^{r} P(L-s)}{1 - \sum_{s=1}^{r} P(L-s) + P(L-r)} \right) - \omega_\beta \, P_1(L,t)
\end{aligned}
\tag{19}
$$

$$
\begin{aligned}
\frac{dP_2(i,t)}{dt} =\ & \left[\omega_{21}^f \, P_1(i-1,t) + \omega_{22}^f \, P_2(i-1,t) \right] \left(\frac{1 - \sum_{s=1}^{r} P(i-1+s)}{1 - \sum_{s=1}^{r} P(i-1+s) + P(i-1+r)} \right) \\
& + \omega_{22}^b \, P_2(i+1,t) \left(\frac{1 - \sum_{s=1}^{r} P(i+1-s)}{1 - \sum_{s=1}^{r} P(i+1-s) + P(i+1-r)} \right) \\
& + \omega_{21} \, P_1(i,t) - \omega_{12} \, P_2(i,t) - \omega_{22}^f \, P_2(i,t) \left(\frac{1 - \sum_{s=1}^{r} P(i+s)}{1 - \sum_{s=1}^{r} P(i+s) + P(i+r)} \right) \\
& - (\omega_{12}^b + \omega_{22}^b) \, P_2(i,t) \left(\frac{1 - \sum_{s=1}^{r} P(i-s)}{1 - \sum_{s=1}^{r} P(i-s) + P(i-r)} \right) \qquad (i \neq L)
\end{aligned}
\tag{20}
$$

$$
\begin{aligned}
\frac{dP_2(L,t)}{dt} =\ & \left[\omega_{21}^f \, P_1(L-1,t) + \omega_{22}^f \, P_2(L-1,t) \right] \left(\frac{1 - \sum_{s=1}^{r} P(L-1+s)}{1 - \sum_{s=1}^{r} P(L-1+s) + P(L-1+r)} \right) \\
& + \omega_{21} \, P_1(L,t) - \omega_{12} \, P_2(L,t) - (\omega_{12}^b + \omega_{22}^b) \, P_2(L,t) \left(\frac{1 - \sum_{s=1}^{r} P(L-s)}{1 - \sum_{s=1}^{r} P(L-s) + P(L-r)} \right) \\
& - \omega_\beta \, P_2(L,t)
\end{aligned}
\tag{21}
$$

B. Steady state properties under open boundary conditions

Using these mean-field equations (17-21) in the steady state, we have numerically calculated our theoretical es-

timates of the flux. These mean-field theoretic estimates are plotted as functions of the rate constants ω_α and ω_{21}^f, respectively, in figs.4(a) and (b). In order to test the level
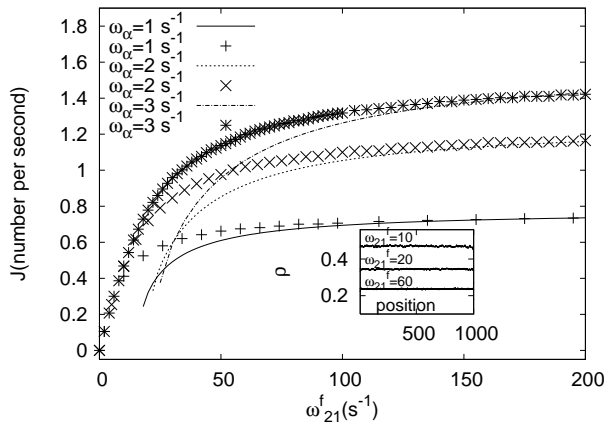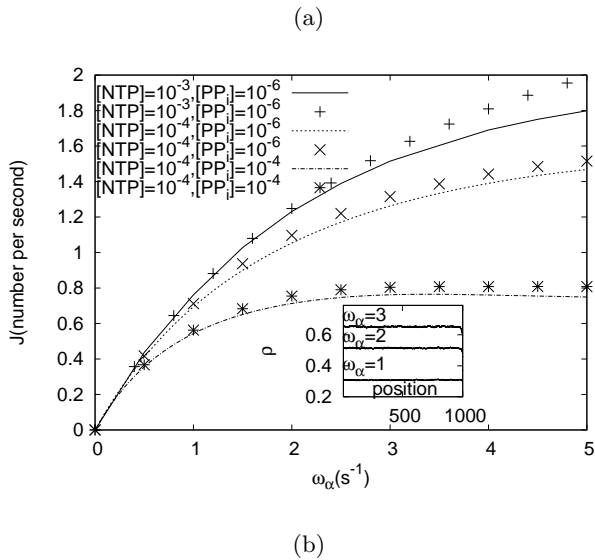
(a)

(b)

(a)

(b)

FIG. 4: The steady-state flux of the RNAPs, under open boundary conditions, plotted as a function of (a) ω_α, for three sets of values of the pair of parameters [NTP], [PP$_i$]; (b) ω_{21}^f for three values of the parameter ω_α. The lines correspond to our mean-field theoretic predictions whereas the discrete data points have been obtained from computer simulations. The insets show the average density profiles for (a) three different values of ω_α and (b) three different values of ω_{21}^f.

of accuracy of these approximate theoretical predictions, we have compared these results with the corresponding numerical data obatined from our direct computer simulations of the model under open boundary conditions. We have also computed the average density profiles and plotted these profiles for three different values of ω_α and three different values of ω_{21}^f in the insets of figs.4(a) and (b), respectively.

The flux increases monotonically with increasing ω_α as well as with increasing ω_{21}^f and, eventually, saturates in both the cases. This trend of variation of flux is accompanied by a monotonic *rise* of the average density profile of the RNAPs in fig.4(a) and with a monotonic *fall* of the average density profile in fig.4(b). A comparison of
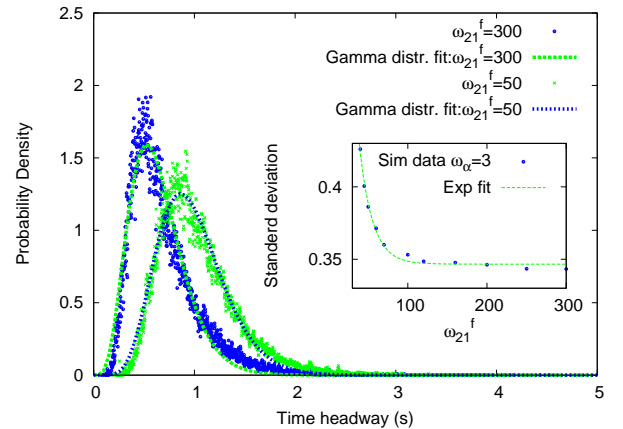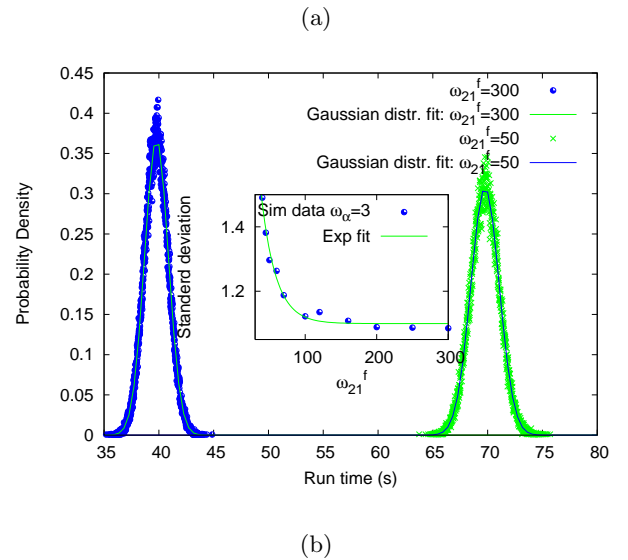
FIG. 5: The distributions of the run times and time headways in our model, under open boundary conditions, plotted in (a) and (b), respectively, for two different values of ω_{21}^f. The discrete data points have been obtained from computer simulations. The curves fitted to these data points are drawn with the lines. The variation of the standard deviations of the distributions of run times and time-headways with the increase of the parameter ω_{21}^f are shown in the insets; the discrete points have been obtained from the simulation data and the best fit curve through these points has been drawn by a line.

these qualitative features of the variation of flux and density profiles with those in ribosome traffic [10], indicates a transition from the low-density phase to the maximal current phase in fig.4(a) and from the high-density phase to the maximal current phase in fig.4(b) [10, 56].
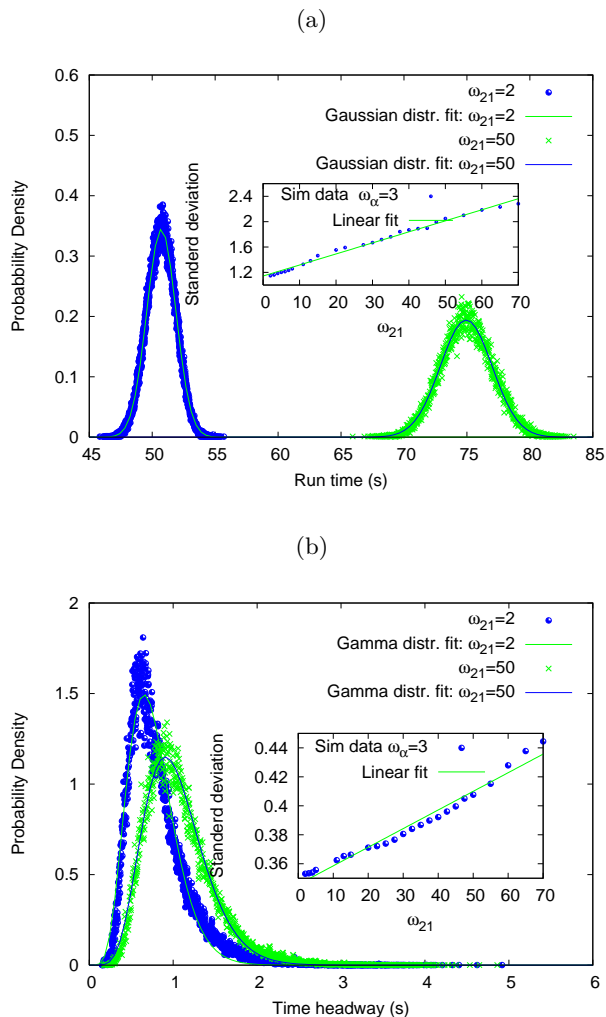
FIG. 6: The distributions of the run times and time-headways in our model, under open boundary conditions, plotted in (a) and (b), respectively, for two different values of ω_{21}. The discrete data points have been obtained from computer simulations. The curves fitted to these data points are drawn with the lines. The variation of the standard deviation of the distributions of run times with the increase of the parameter ω_{21} are shown in the insets; the discrete points have been obtained from the simulation data and the best fit curve through these points has been drawn by a line.

VI. RNAP-TO-RNAP FLUCTUATIONS AND TRANSCRIPTIONAL NOISE

The distribution $\tilde{P}_T$ of run times T is a measure of the RNAP-to-RNAP fluctuations in the rates of transcription. This distribution, obtained from computer simulations of our model, is plotted in fig.5(a) for two different values of the parameter ω_{21}^f. The gaussian fit to the distribution $\tilde{P}_T$ is consistent with the gaussian distributions of the "delay times" obtained by Morelli and Jülicher [57] in the limit of sufficiently large number of intermediate steps. Gaussian distributions of the speeds of the RNAPs were observed by Tolic-Norrelykke et al.[58] in their *in-vitro* experiments. Although this conclusion in ref.[58] was based on the assumption of uniform speed of the RNAPs during the elongation stage, what was actually observed in their experiments is the Gaussian distribution of the run times; this is certainly consistent with our theorertical result.

We define the standard deviation, i.e., the root-mean-square deviations

$$\eta_T = < (T - <T>)^2 >^{1/2} \tag{22}$$

of run times T from their mean, as a measure of the transcriptional noise arising from the stochastic mechano-chemical cycles of the RNAPs. η_T is plotted as a function of ω_{21}^f in the inset of fig.5(a). Since $\omega_{21}^f = \omega_{21}^{f0}[NTP]$, the inset of fig.5(a) clearly establishes that the transcriptional noise η_T falls exponentially with increasing concentration of NTP. This trend of variation is consistent with the well known fact that the fluctuations in the rates of chemical synthesis are stronger when the concentrations of reactants are lower.

The distribution $\mathcal{P}_\tau$ of time-headways τ is a measure of the fluctuations in the time interval between the completion of the polymerization of successive mRNA transcripts. This distribution, also obtained from computer simulations of our model, is plotted in fig.5(b) for the same values of the ω_{21}^f as those used in fig.5(a). The best fit to the numerical data for $\mathcal{P}_\tau$ is of the general form

$$\mathcal{P}_\tau = C\tau^\nu e^{-\mu\tau} \tag{23}$$

with positive constants μ and ν; C being the normalization constant. The form (23) is consistent with the gamma distribution that is expected for the time-headways at suffciently low densities.

We define

$$\eta_\tau = < (\tau - <\tau>)^2 >^{1/2} \tag{24}$$

as a measure of the fluctuations in the time-headways. In the inset of fig.5(b) we plot η_τ as a function of ω_{21}^f; the best fit to this curve is an exponential.

In the limit in which $\omega_{12} \to \infty$ and all other rate constants, except $\omega_{21}^f = q$, vanish, our model reduces to TASEP if, simultaneously $r \to 1$. In this limit of our model $\mathcal{P}_\tau$ is expected to be well approximated by the exact expression for TASEP with *parallel* updating [59, 60]:

$$\mathcal{P}_\tau = \left[\frac{qy}{\rho - y}\right]\{1 - (qy/\rho)\}^{t-1} + \left[\frac{qy}{(1-\rho) - y}\right]\{1 - (qy/(1-\rho))\}^{t-1} - \left[\frac{qy}{\rho - y} + \frac{qy}{(1-\rho) - y}\right]p^{t-1} - q^2(t-1)p^{t-2}.$$

(25)

where

$$y = \frac{1}{2q}\left(1 - \sqrt{1 - 4q\rho(1-\rho)}\right). \qquad (26)$$

Finally, the transcriptional noise increases, instead of decreasing, with the increase of PP_i concentration (see fig.6); in other words, increase of PP_i concentration not only slows down the average rate of RNA synthesis, but also makes transcription more noisy.

VII. IMPLICATIONS FOR EXPERIMENTS

Almost all the quantitative theories of RNAP developed so far [25, 26, 27, 28, 29, 30, 31, 32, 33, 34, 35] were intended to account for the mechano-chemistry of a *single* RNAP. The interactions of RNAPs in transcriptional interference [61] is a well known phenomenon and it has also been modelled quantitatively [39]. However, instead of studying interactions of RNAPs during the transcription of different genes [36, 37, 38, 39], we have modelled the steric interactions of RNAPs which are simultaneously involved in the transcription of the same gene.

The possibility of steric interactions of RNAPs during their traffic-like collective movements along the same DNA template has been known for a long time [62, 63]. The "christmas-tree"-like structures [64, 65] observed in electron microscopic studies of eukaryotic transcription arise from simultaneous transcription of the same gene by many RNAPs. These structures also have strong similarity with the dense population of the nascent mRNA transcripts observed all along the loops of the DNA strands in the electron micrographs of lampbrush chromosomes [66, 67].

Our theory predicts not only the average rate of synthesis of RNA, but also two different measures of fluctuations in the process of transcription. In most of the earlier experimental investigations of transcriptional noise, the distributions of the sizes and frequencies of the "burst" of the transcriptional activity were recorded. However, size and frequency of the bursts depend on the temporal resolution used for *sorting* the time series of the events into separate bursts (see, for example, Fig.1 of ref.[68]). Therefore, in principle, the statistics of reported distributions of burst sizes and frequencies may change with the change of time resolution selected for such sorting. Instead, in this paper, we have introduced new measures of the stochasticity in transcriptional activity which do not require any sorting of this kind.

In recent years sophisticated optical techniques have been developed for single mRNA imaging [69, 70, 71, 72]. We believe that our theoretical predictions can be tested most appropriately by carrying out *in-vitro* experiments with either fluorescently labelled RNAPs [58] or using techniques for tagging the nascent mRNA with fluorescent probes [44, 69] or using techniques where fluorescent probes can quickly bind with the nascent mRNA as soon as it is released by the RNAP [45]. Comparison of our theoretical predictions on the distributions of run times and time headways require collection of appropriate data. In our theory, the run time includes the time spent by a RNAP in the elongation stage as well as in the termination stage, but does not include the time spent in the initiation stage. Therefore, in experiments, run times of the RNAps should be measured only from the instant when the TEC gets stabilized; a technique used in ref.[58] may be utilized for this purpose.

VIII. SUMMARY AND CONCLUSIONS

Surprisingly, no attempt has been made in the past to develope mathematical models for RNAP traffic where transcription of a single gene is carried out simultaneously by a stream of RNAPs closely spaced on the same DNA template. To our knowledge, the model developed in this paper is the first attempt to capture inter-RNAP interactions in a model where the mechano-chemical cycles of each individual RNAPs in the elongation stage are also incorporated, albeit in a simplified manner. In analogy with vehicular traffic [41], we have defined the flux for RNAP traffic; the RNAP flux is also the total rate of synthesis of RNA. We have calculated the average rates of RNA synthesis analytically under mean-field approximation. For the sake of ease of analytical calculations, throughout this paper we have assumed a hypothetical homogeneous sequence of nucleotides on the ssDNA template. But, our model can be easily extended to capture inhomogeneous sequences of real DNA although, in such realistic situations, only numerical calculations will be possible.

Drawing analogies with vehicular traffic, we have defined two novel quantities whose distributions serve as measures of RNAP-to-RNAP fluctuations in the transcription of a single gene. We have calculated these distributions numerically by carrying out computer simulations of our model. The widths of these distributions (more precisely, root-mean-square fluctuations)

can be treated as good measures of the strength of "transcriptional noise". We have investigated how the level of "transcriptional noise" depends on some of the model parameters which can be varied in a controlled manner in laboratory experiments. A similar analysis of "translational noise", which arises from ribosome-to-ribosome fluctuations during protein synthesis from the same mRNA template, will be reported elsewhere [73]. The inhomogeneous sequence of nucleotides on the DNA template can lead to stronger fluctuations thereby making additional contributions to the levels of transcriptional noise. The "intrinsic noise" studied in this paper arises from the stochastic nature of the steps of the mechano-chemical cycle of individual RNAPs. Although the nois level gets affected by the interactions of the RNAPs, this noise remains relevant even when the gene is transcribed by one RNAP at a time. We have made concrete suggestions as to the experimental systems and techniques which, in principle, can be used to test our theoretical predictions.

[1] M. Schliwa, (ed.) *Molecular Motors*, (Wiley-VCH, 2003).
[2] D. D. Hackney and F. Tanamoi, *The Enzymes*, vol.XXIII *Energy Coupling and Molecular Motors* (Elsevier, 2004).
[3] A.B. Kolomeisky and M.E. Fisher, in: *Annual Review of Physical Chemistry*, **58**, 675 (2007).
[4] D. Chowdhury, A. Schadschneider and K. Nishinari, Phys. of Life Rev. **2**, 318 (2005).
[5] Special issue 1 of vol. **372** of Physica A, on "common trends in traffic systems" guest eds. D. Chowdhury, B. K. Chakrabarti and A. Dutta (2006).
[6] R. Lipowsky, Y. Chai, S. Klumpp, S. Liepelt and M. J.I. Mller, Physica A (2006) in press and references therein.
[7] E. Frey, A. Parmeggiani and T. Franosch, Genome Inf. **15**, 46 (2004) and references therein.
[8] M.R. Evans, R. Juhasz and L. Santen, Phys. Rev. E **68**, 026117 (2003).
[9] V. Popkov, A. Rakos, R.D. Williams, A.B. Kolomeisky and G.M. Schütz, Phys. Rev. E **67**, 066117 (2003).
[10] A. Basu and D. Chowdhury, Phys. Rev. E **75**, 021902 (2007)
[11] K. Nishinari, Y. Okada, A. Schadschneider and D. Chowdhury, Phys. Rev. Lett. **95**, 118101 (2005).
[12] P. Greulich, A. Garai, K. Nishinari, A. Schadschneider and D. Chowdhury, Phys. Rev. E **75**, 041905 (2007).
[13] L. Bai, T.J. Santangelo and M.D. Wang, Annu. Rev. Biophys. Biomol. Str. **35**, 343 (2006).
[14] J. Gelles and R. Landick, Cell, **93**, 13 (1998).
[15] N. Korzheva and A. Mustaev, in ref.[1].
[16] C. MacDonald, J. Gibbs and A. Pipkin, Biopolymers **6**, 1 (1968).
[17] C. MacDonald and J. Gibbs, Biopolymers, **7**, 707 (1969).
[18] G. Lakatos and T. Chou, J. Phys. A **36**, 2027 (2003).
[19] L.B. Shaw, R.K.P. Zia and K.H. Lee, Phys. Rev. E **68**, 021910 (2003).
[20] L.B. Shaw, J.P. Sethna and K.H. Lee, Phys. Rev. E **70**, 021901 (2004).
[21] L.B. Shaw, A.B. Kolomeisky and K.H. Lee, J. Phys. A **37**, 2105 (2004).
[22] T. Chou, Biophys. J., **85**, 755 (2003).
[23] T. Chou and G. Lakatos, Phys. Rev. Lett. **93**, 198101 (2004).
[24] J.J. Dong, B. Schmittmann and R.K.P. Zia, J. Stat. Phys. **128**, 21 (2007).
[25] F. Jülicher and R. Bruinsma, Biophys. J. **74**, 1169 (1998).
[26] H.Y. Wang, T. Elston, A. Mogilner and G. Oster, Biophys. J. **74**, 1186 (1998).
[27] R. Sousa, Trends in Biochem. Sci. **21**, 186 (1996).
[28] R. Guajardo and R. Sousa, J. Mol. Biol. **265**, 8 (1997).
[29] Q. Guo and R. Sousa, J. Mol. Biol. **358**, 241 (2006).
[30] L. Bai, A. Shundrovsky and M.D. Wang, J. Mol. Biol. **344**, 335 (2004).
[31] L. Bai, R.M. Fulbright and M.D. Wang, Phys. Rev. Lett. **98**, 068103 (2007).
[32] G. Bar-Nahum, V. Epshtein, A.E. Ruckenstein, R. Rafikov, A. Mustaev and E. Nudler, Cell **120**, 183 (2005).
[33] V.R. Tadigotla, D.O. Maoileidigh, A.M. Sengupta, V. Epshtein, R.H. Ebright, E. Nudler and A.E. Ruckenstein, Proc. Nat. Acad. Sci. USA, **103**, 4439 (2006).
[34] Y. R. Yamada and C.S. Peskin, arxiv:q-bio.BM/0603012 (2006).
[35] H.J. Woo, Phys. Rev. E **74**, 011907 (2006).
[36] V. Epshtein and E. Nudler, Science **300**, 801 (2003).
[37] V. Epshtein, F. Toulme, A. Rachid Rahmouni, S. Borukhov and E. Nudler, EMBO J. **22**, 4719 (2003).
[38] N. Crampton, W.A. Bonass, J. Kirkham, C. Rivetti and N.H. Thomson, Nucleic Acids Research, **34**, 5416 (2006).
[39] K. Sneppen, I.B. Dodd, K.E. Shearwin, A.C. Palmer, R.A. Schubert, B.P. Callen and J.B. Egan, J. Mol. Biol. **346**, 399 (2005).
[40] H. Bremer and M. Ehrenberg, Biochim. Biophys. Acta **1262**, 15 (1995).
[41] D. Chowdhury, L. Santen and A. Schadschneider, Phys. Rep. **329**, 199 (2000).
[42] M. Kaern, T.C. Elston, W. J. Blake and J.J. Collins, Nat. Rev. Genetics **6**, 451 (2005).
[43] J. Paulsson, Phys. of Life Rev. **2**, 157 (2005).
[44] I. Golding, J. Paulsson, S.M. Zawilski and E.C. Cox, Cell **123**, 1025 (2005).

[45] A. Raj, C.S. Peskin, D. Tranchina, D.Y. Vargas and S. Tyagi, PloS Biol. **4**, 1707 (2006).

[46] J.R. Chubb, T. Trcek, S.M. Shenoy and R.H. Singer, Curr. Biol. **16**, 1018 (2006).

[47] X. Darzacq, Y. Shav-Tal, V. de Turris, Y. Brody, S.M. Shenoy, R.D. Phair and R.H. Singer, Nat. Str. & Mol. Biol. doi:10.1038/nsmb1280. (2007).

[48] S.M. Uptain, C.M. Kane and M.J. Chamberlin, Annu. Rev. Biochem. **66**, 117 (1997).

[49] P. Cramer, Curr. Op. in Str. Biol. **12**, 89 (2002).

[50] K.J. Armache, H. Kettenberger and P. Cramer, Curr. Op. Str. Biol. **15**, 197 (2005).

[51] D.A. Erie, T.D. Yager and P.H. von Hippel, Annu. Rev. Biophys. and Biomol. Str. **21**, 379 (1992).

[52] P.H. von Hippel, Science **281**, 660 (1998)

[53] S.J. Greive and P.H. Von Hippel, Nat. Rev. Mol. Cell Biol. **6**, 221 (2005).

[54] E.A. Abbondanzieri, W.J. Greenleaf, J.W. Shaevitz, R. Landick and S.M. Block, Nature, **438**, 460 (2005).

[55] E.A. Galburt, S. W. Grill, A. Wiedmann, L. Lubkowska, J. Choy,E. Nogales, M. Kashlev and C. Bustamante, Nature **446**, 820 (2007).

[56] G. M. Schütz, in: *Phase Transitions and Critical Phenomena*, vol. 19 (Acad. Press, 2001).

[57] L. G. Morelli and F. Jülicher, Phys. Rev. Lett. **98**, 228101 (2007).

[58] S.F. Tolic-Norrelykke, A.M. Engh, R. Landick and J. Gelles, **279**, 3292 (2004).

[59] K. Ghosh, A. Majumdar and D. Chowdhury, Phys. Rev. E **58**, 4012 (1998).

[60] D. Chowdhury, A. Pasupathy and S. Sinha, Eur. Phys. J. B **5**, 781 (1998).

[61] K.E. Shearwin, B.P. Callen and J.B. Egan, Trends in Genetics **21**, 339 (2005).

[62] B. Alberts, D. Bray, K. Hopkin, A. Johnson, J. Lewis, M. Raff, K. Roberts and P.Walter, *Essential Cell Biology*, 2nd ed. (Garland Science, Taylor and Francis, 2004).

[63] D.A. Jackson, F.J. Iborra, E.M.M. Manders and P.R. Cook, Mol. Biol. of the Cell **9**, 1523 (1998).

[64] U. Scheer, B. Xia, H. Merkert and D. Weisenberger, Chromosoma **105**, 470 (1997).

[65] I. Raska, K. Koberna, J. Malinsky, H. Fidlerova and M. Masata, Biol. of the Cell **96**, 579 (2004).

[66] H. G. Callan, *Lampbrush Chromosomes*, (Springer, Berlin, 1986).

[67] J. G. Gall, Nat. Med. **12**, 1142 (2006).

[68] I. Golding and E.C. Cox, Curr. Biol. **16**, R371 (2006).

[69] Y. Shav-Tal, R.H. Singer and X. Darzacq, Nat. Rev. Mol. Cell Biol. **5**, 856 (2004).

[70] A.J. Rodriguez, J. Condeelis, R.H. Singer and J.B. Dictenberg, Seminars in Cell & Dev. Biol. **18**, 202 (2007).

[71] X. Darzacq, Y. Shav-Tal and R.H. Singer, in: *New Frontiers in Ultrasensitive Bioanalysis*, ed. Xiao-Hong Nancy Xu (John Wiley, 2007).

[72] I. Golding and E.C. Cox, Phys. Rev. Lett. **96**, 098102 (2006).

[73] A. Garai et al. (to be published).